Behavioral/Systems/Cognitive

Multisegmental Aδ- and C-Fiber Input to Neurons in Lamina I and the Lateral Spinal Nucleus

Vítor Pinto,[1,2] Peter Szucs,[1] Deolinda Lima,[2] and Boris V. Safronov[1,2]

[1]Instituto de Biologia Molecular e Celular, Universidade do Porto, 4150-180 Porto, Portugal, and [2]Laboratório de Biologia Celular e Molecular, Faculdade de Medicina, Universidade do Porto, 4200-319 Porto, Portugal

Spinal lamina I and the lateral spinal nucleus (LSN) receive and integrate nociceptive primary afferent inputs to project through diverse ascending pathways. The pattern of the afferent supply of individual lamina I and LSN neurons through different segmental dorsal roots is poorly understood. Therefore, we recorded responses of lamina I and LSN neurons in spinal segments L4 and L3 to stimulation of six ipsilateral dorsal roots (L1–L6). The neurons were viewed through the overlying white matter in the isolated spinal cord preparation using the oblique infrared LED illumination technique. Orientation of myelinated fibers in the white matter was used as a criterion to distinguish between the LSN and lamina I. Both types of neurons received mixed (monosynaptic and polysynaptic) excitatory Aδ- and C-fiber input from up to six dorsal roots, with only less than one-third of it arising from the corresponding segmental root. The largest mixed input arose from the dorsal root of the neighboring caudal segment. Lamina I and LSN neurons could fire spikes upon the stimulation of up to six different dorsal roots. We also found that individual lamina I neurons can receive converging monosynaptic Aδ- and/or C-fiber inputs from up to six segmental roots. This study shows that lamina I and LSN neurons function as intersegmental integrators of primary afferent inputs. We suggest that broad monosynaptic convergence of Aδ- and C-afferents onto a lamina I neuron is important for the somatosensory processing.

Introduction

Spinal lamina I processes diverse modalities of nociceptive input and projects through ascending tracts to different areas of the brainstem and thalamus (Lima and Almeida, 2002). Lamina I neurons receive inputs from thin afferents innervating skin, joints, muscles, and viscera (Cervero and Connell, 1984a,b; Dostrovsky and Craig, 2006). The central branches of thin afferents entering the superficial dorsal horn terminate not only in the segment of root entrance but also one to two segments above and below (Szentagothai, 1964; Cruz et al., 1987). These studies indicated that neurons in the same segment can receive afferents from different roots. Indeed, it has recently been shown that single lamina II neurons receive converging monosynaptic Aδ- and C-fiber inputs from several roots and that this can be important for both the sensory integration and the formation of robust and precise somatotopic maps (Pinto et al., 2008b). Although a number of *in vivo* unit recording studies have examined the afferent input to lamina I neurons (Kumazawa and Perl, 1978; Woolf and Fitzgerald, 1983), the pattern of multisegmental convergence of Aδ- and C-fiber input to lamina I neurons remains unknown.

The lateral spinal nucleus (LSN) is located within the dorsolateral funiculus in the rat spinal cord (Gwyn and Waldron, 1968, 1969). The LSN differs from the superficial dorsal horn in the nature of its neuropil, where the cell bodies are found surrounded by the rostrocaudally oriented myelinated axons. LSN neurons project through ascending tracts to the brainstem, hypothalamus, and thalamus (Menétrey et al., 1982; Pechura and Liu, 1986; Menétrey and Basbaum, 1987; Leah et al., 1988; Burstein et al., 1990a,b) and can be activated by noxious stimulation (Olave and Maxwell, 2004). However, little is known about the afferent inputs to the LSN. LSN neurons are not directly activated by cutaneous stimulation (Giesler et al., 1979; Menétrey et al., 1980) but respond to movement of joints and deep tissue (Menétrey et al., 1980). For this reason, the afferent input to the LSN is associated with C-fibers innervating muscles (Olave and Maxwell, 2004) and viscera (Sugiura et al., 1989). To our knowledge, there are no reports describing the responses of LSN neurons to stimulation of dorsal roots.

One reason why the complex pattern of afferent supply of lamina I and LSN neurons has not been previously described is the lack of an adequate experimental approach. However, the recent development of imaging techniques has enabled visualization of intact lamina I neurons for the tight-seal recordings in the isolated spinal cord with attached dorsal roots (Safronov et al., 2007; Szucs et al., 2009). The neurons visualized through the overlying white matter preserved both their dendritic structure and primary afferent input. Furthermore, organization of the myelinated fibers in the dorsolateral white matter could be used for identification of lamina I and LSN neurons.

Here we studied monosynaptic and polysynaptic responses of individual lamina I and LSN neurons to stimulation of six ipsi-

Received July 17, 2009; revised Dec. 22, 2009; accepted Dec. 24, 2009.

This work was supported by a grant from the Portuguese Foundation for Science and Technology funded by POCTI2010 and Fundo Europeu de Desenvolvimento Regional (FEDER). We thank Nuno Sousa for providing the Neurolucida system.

Correspondence should be addressed to Boris V. Safronov, Instituto de Biologia Molecular e Celular, Universidade do Porto, Rua do Campo Alegre 823, 4150-180 Porto, Portugal. E-mail: safronov@ibmc.up.pt.

DOI:10.1523/JNEUROSCI.3445-09.2010

 0270-6474/10/302384-12$15.00/0

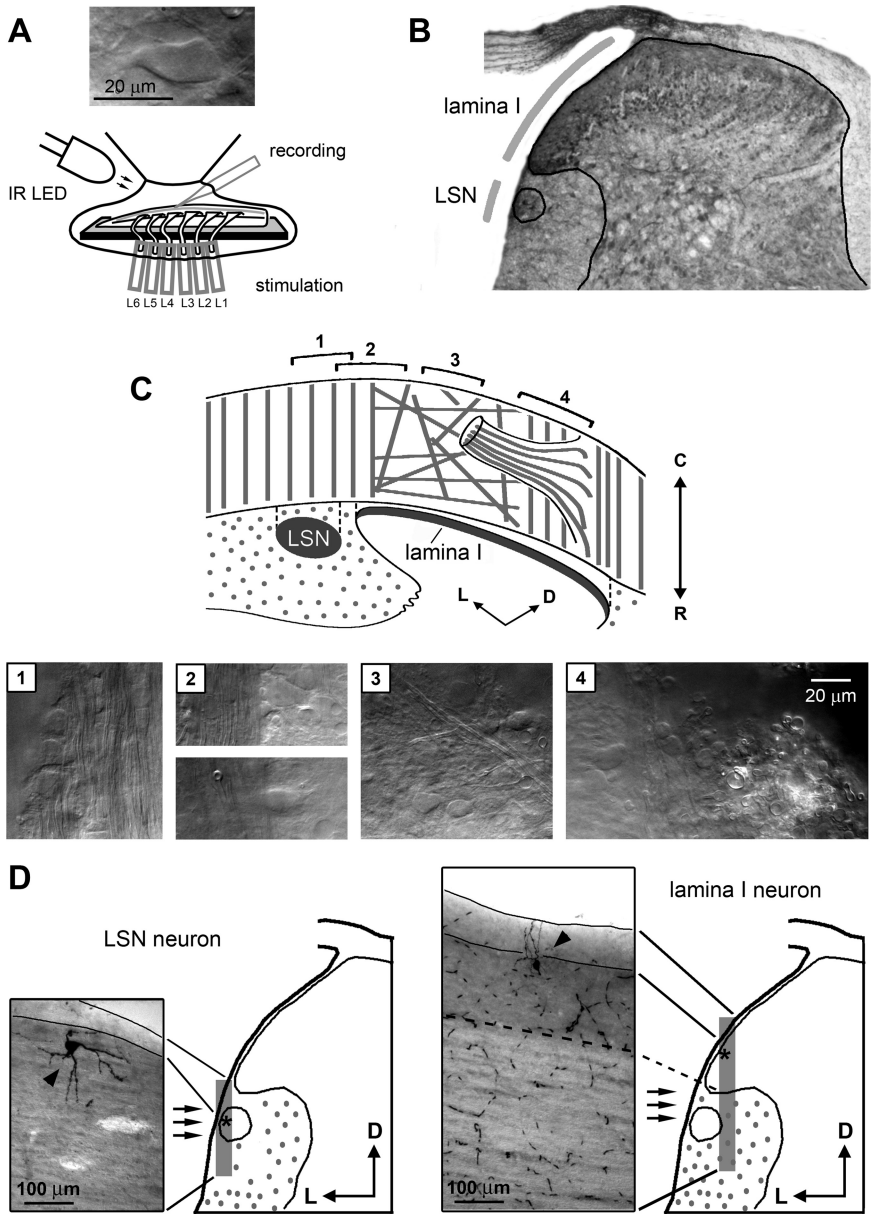

Figure 1. Identification of lamina I and LSN neurons in the isolated spinal cord. ***A***, Preparation of the lumbar spinal cord with unilateral six dorsal roots, L1–L6. The roots were stimulated through suction electrodes. Inset, Lamina I neuron viewed using oblique LED illumination. ***B***, A cross section of the fixed spinal cord (L4, 27-d-old rat) with indications of the LSN and the lamina I region accessible for the recording. Continuous lines show the border of the gray matter and the LSN. ***C***, Schematic drawing of the fiber orientation in the dorsal and dorsolateral white matter used for the identification of the LSN and lamina I. The photographs shown below were taken from the regions (1–4) indicated on the schematic drawing. The focal plane was chosen to show the fibers. Region 1, The LSN: large neuronal cell bodies are surrounded by the parallel rostrocaudal myelinated fibers of the dorsolateral funiculus. Region 2, Transitional zone between the dorsolateral funiculus (left) and lamina I (right). Region 3, Network of the randomly oriented fibers and the scattered cell bodies in lamina I. Region 4, The medial border of accessible part of lamina I (left) and myelinated fibers in the dorsal root entry zone (right). ***D***, Parasagittal sections (100 μm thick) of the spinal cord with a biocytin-labeled LSN neuron (left) and lamina I neuron (right). Locations of the sections are shown in the schematic drawings where asterisks indicate the cell body positions. Left, LSN neuron is found outside the spinal gray matter within the dorsolateral funiculus. Continuous lines show the dorsal borders of the white matter in the top and bottom of the section. Right, Lamina I neuron is seen within the dorsolateral gray matter. Dashed line shows the border between the gray and white matter. Continuous lines indicate the dorsal borders of the white matter in the top and bottom of the section.

lateral dorsal roots. We found that both types of neuron function as intersegmental integrators of primary afferent input. Our data suggest that broad convergence of afferents onto a lamina I neuron is important for the somatosensory processing.

Materials and Methods

Preparation of the spinal cord with six roots. Laboratory Wistar rats (2–5 weeks old) of either sexes were killed in accordance with the national guidelines (Direcção Geral de Veterinária, Ministério da Agricultura) after anesthesia with intraperitoneal injection of Na^+-pentobarbital (30 mg/kg) and subsequent check for lack of pedal withdrawal reflexes. The vertebral column was quickly cut out and immersed in oxygenated artificial CSF (ACSF) at room temperature. The vertebral column was opened from its ventral side with scissors, and the lumbar spinal cord with unilateral L1–L6 dorsal roots was dissected. The pia mater was locally removed in the region of interest with forceps and scissors to provide access for the recording pipette. The spinal cord was glued with cyanoacrylate adhesive to a golden plate (the dorsolateral spinal cord surface was up) and transferred to the recording chamber (Fig. 1*A*). All measurements were done at 22–24°C.

Identification of lamina I and LSN neurons. Lamina I and LSN neurons were visualized (Fig. 1*A*) through the intact dorsolateral white matter in the lumbar spinal cord using the oblique infrared LED illumination technique (Pinto et al., 2008b; Szucs et al., 2009). Identification of the neurons was based on orientation of myelinated fibers in the dorsolateral white matter and was confirmed by morphological analysis of biocytin-labeled neurons. Lamina I neurons were identified in the dorsal gray matter lateral to the dorsal root entry point, in the region indicated in Figure 1*B*. The white matter in this region is thin in young animals and has virtually no ascending/descending primary afferent fibers (Pinto et al., 2008b). The neurons in the dorsal gray matter medial to the dorsal root entry point were not accessible for tight-seal recordings because of the thick dorsal white matter formed by ascending/descending afferents (Pinto et al., 2008b). The fraction of lamina I inaccessible for recording changed with age, being smaller in younger animals. The LSN was found near to the spinal cord surface and was separated by the white matter from lamina I (Fig. 1*B*).

A schematic drawing of the fiber orientation together with the fiber images used for the identification of lamina I and the LSN is shown in Figure 1*C*. At the lateral border of lamina I (region 2), a clear transition between the dorsolateral funiculus (left) and lamina I (right) was seen. In this transitional zone, the dorsolateral funiculus appeared as a bundle of densely packed parallel rostrocaudal myelinated fibers free of cell bodies. In contrast, lamina I was devoid of parallel fibers but possessed large cell bodies of superficial neurons (Fig. 1*C*, region 2, bottom). Laterally to this transitional zone, the LSN was seen as a column of numerous cell bodies surrounded by the parallel myelinated fibers (region 1). Medial to the transitional zone, lamina I appeared as a network of randomly oriented fibers and dispersed cell bodies (region 3). Near to the dorsal root entry point, the bundles of ascending/descending primary afferent fibers forming the dorsal white matter demarcated the medial border of lamina I

Table 1. Converging monosynaptic inputs to L4 and L3 lamina I neurons

Cell	Firing type	L1 Aδ	L1 C	L2 Aδ	L2 C	L3 Aδ	L3 C	L4 Aδ	L4 C	L5 Aδ	L5 C	L6 Aδ	L6 C	Input from roots	Converging roots
Lamina I neuron in L4															
1	DFN	○	—	○	—	○	—	○	*	*	*	*	*	4Aδ	4
2	TFN	—	—	○	—	○	*	○	*	*	*	—	*	3Aδ	3
3	TFN	—	—	—	—	○	—	○	—	○	*	*	*	3Aδ	3
4	TFN	—	—	—	—	—	—	○	—	○	*	○	—	3Aδ	3
5	DFN	—	—	○	—	—	—	○	*	○	●	*	—	3Aδ + 1C	3
6	TFN	—	—	○	●	—	—	—	—	○	*	○	●	3Aδ + 2C	3
7	TFN	—	●	—	●	○	—	○	—	○	●	○	*	4Aδ + 3C	6
8	TFN	—	*	*	*	*	●	*	*	○	*	—	*	1Aδ + 1 C	2
9	TFN	—	—	—	●	—	●	○	*	○	*	—	*	2Aδ + 2C	4
10	TFN	—	—	*	*	—	*	○	*	*	●	○	●	2Aδ + 2C	3
11	TFN	—	—			—	—	—	●	—	●	—	—	2C	2
Lamina I neuron in L3															
12	TFN	—	—	○	—	○	*	○	*	○	—	*	—	4Aδ	4
13	DFN	—	—	—	—	○	—	○	—	○	—	—	—	3Aδ	3
14	TFN	—	—	—	—	—	—	○	*	○	*	—	—	2Aδ	2
15		—	●	○	—	○	—	○	—	○	—	*	*	4Aδ + 1C	5
16	DFN	—	—	—	—	○	*	○	●	○	*	○	*	4Aδ + 1C	4
17	TFN	—	—	○	●	*	*	○	*	○	*	—	—	3Aδ + 1C	3
18	TFN	—	—	—	—	*	●	○	—	—	—	—	—	1Aδ + 1C	2
19	TFN	—	●			*	●	○	*	*	●	—	*	1Aδ + 3C	4
20	TFN	—	—	—	●	—	●	—	●	—	●	—	—	4C	4

This table describes only those lamina I neurons for which the monosynaptic inputs from at least two segmental dorsal roots could be confirmed. Monosynaptic Aδ- and C-fiber inputs are indicated by open and filled circles, respectively. Asterisks (*) indicate inputs from segmental roots that could not be analyzed due to large number of overlapping EPSCs. — indicates inputs from roots that were analyzed, but the monosynaptic EPSCs were not revealed. In cells 11 and 19, the L2 roots were damaged. In the last but one column, the input from the roots is given as n_1Aδ + n_2C, where n_1 and n_2 are the numbers of different segmental dorsal roots with monosynaptic Aδ- and C-fiber projections, respectively. In the last column, the number of converging roots is the number of segmental dorsal roots with monosynaptic Aδ-/C-inputs. TFN, Tonic-firing neuron; DFN, delayed-firing neuron. The firing pattern in cell 15 could not be identified.

accessible for recordings (region 4). Lamina I neurons could be clearly distinguished from deeper located lamina II neurons whose somata were smaller and appeared as a densely packed cell layer (Szucs et al., 2009).

Cell filling, processing, and reconstruction. In 47 experiments, neurons were labeled by including biocytin (0.5%) in the pipette solution. Labeled neurons were revealed and reconstructed as described previously (Pinto et al., 2008b; Szucs et al., 2009). After fixation in 4% paraformaldehyde, the spinal cord was embedded in agar and parasagittal serial sections (thickness, 100 μm) were prepared with a tissue slicer (Leica, VT 1000S). To reveal biocytin, the sections were permeabilized with 50% ethanol and treated according to the avidin-biotinylated horseradish peroxidase method (ExtrAvidin-Peroxidase, diluted 1:1000) followed by a diaminobenzidine chromogen reaction. Sections were counterstained with 1% toluidine blue to determine borders of the gray matter and laminae during reconstruction. Photomicrographs were taken with a Primo Star (Zeiss) microscope equipped with a Guppy (Allied Vision Technologies) digital camera. Contrast and brightness of the images used for the figures were adjusted using Adobe Image Ready software.

Reconstructions were done from serial sections. A window of the Neurolucida software (MBF Bioscience, review version) was dimmed and superimposed on the live digital image of the section (objective, 40×) by means of the Transparent Windows 2.2 application. All dendrites, somata, and axons as well as contours of the gray and white matter were completely traced into a serial section data file in two dimensions. During the reconstruction, the

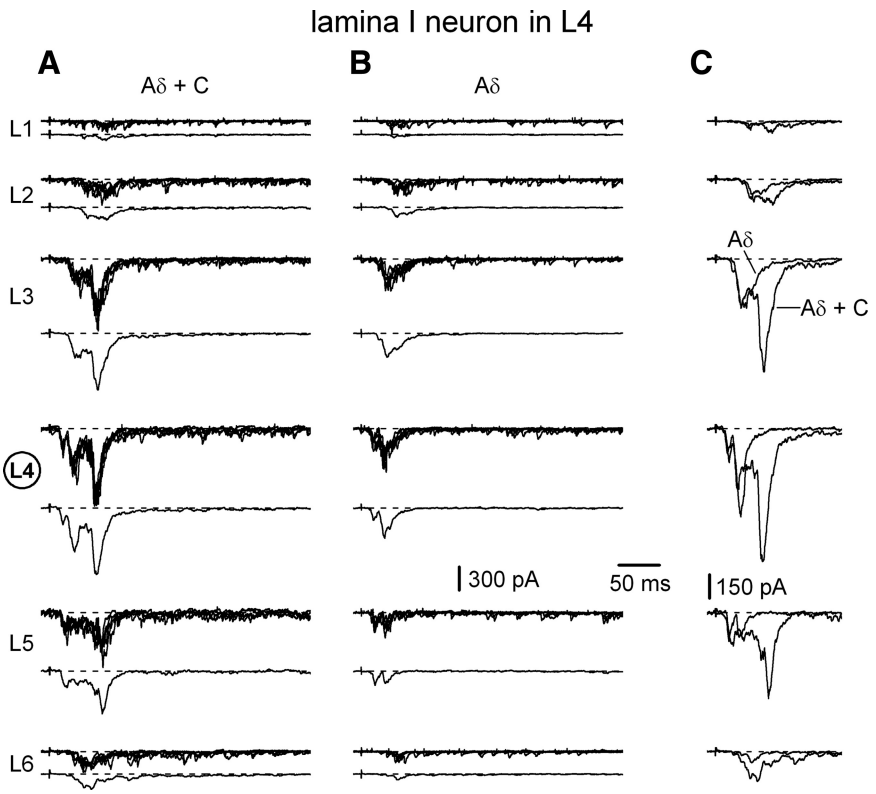

Figure 2. Mixed inputs to an L4 lamina I neuron. Mixed (monosynaptic and polysynaptic) EPSCs were elicited in an L4 lamina I neuron by stimulating L1–L6 roots. ***A***, Each root was stimulated at least 10 times with a 1 ms current pulse at 0.1 Hz to elicit both Aδ- and C-fiber mixed EPSCs. For each root, individual recordings (upper traces) were averaged (lower traces). ***B***, Each dorsal root was stimulated at least 10 times with a 50 μs pulse at 1 Hz to elicit only Aδ-fiber mixed EPSCs. Averaged responses (lower traces) were obtained from individual recordings (upper traces). ***C***, The averaged traces are shown superimposed. Holding potential was −70 mV. Here and in the following figures, the fastest evoked EPSCs (monosynaptic and polysynaptic) appeared with latencies corresponding to afferent conduction velocity below 4.4 m/s (conduction velocity of the fastest Aδ-afferents in dorsal roots, Pinto et al., 2008a). Note that all roots differed in length, and therefore, had different latency criteria for separation of Aδ- and C-fiber EPSCs.

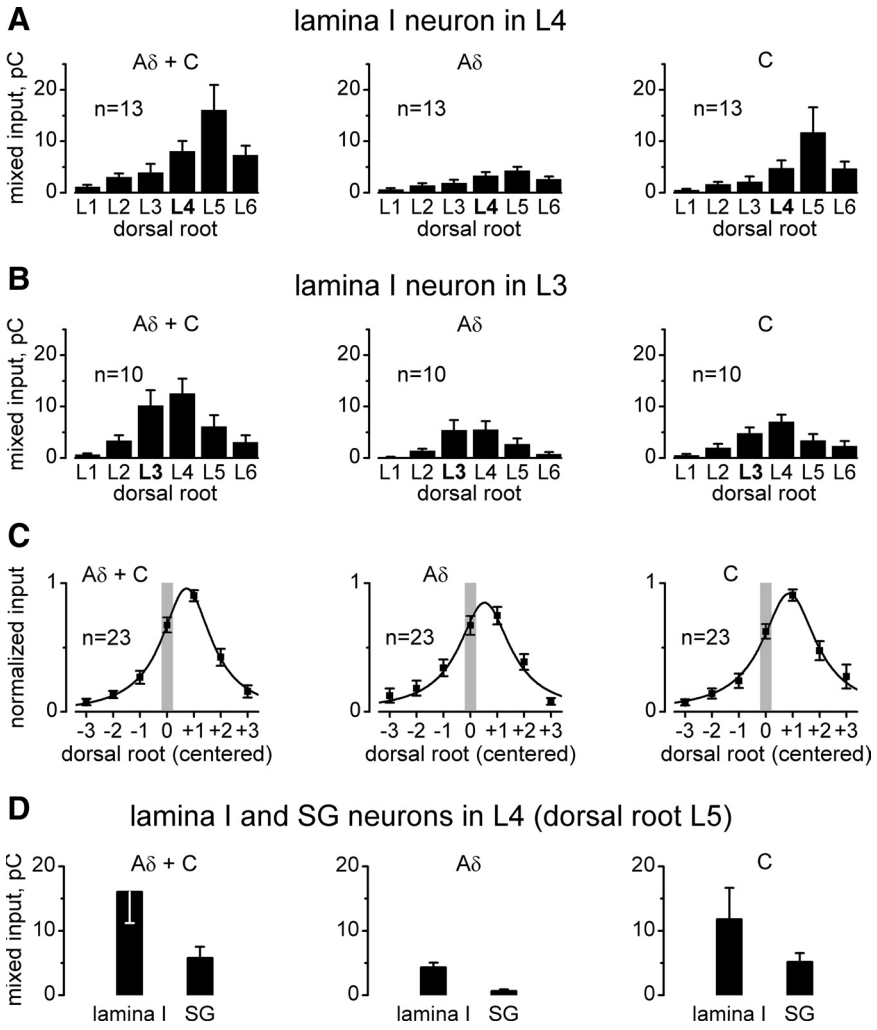

Figure 3. Integrated mixed inputs to lamina I neurons. ***A***, integrated mixed inputs to an L4 lamina I neuron from L1–L6 roots. For each root, the areas under the corresponding averaged traces (similar to those in Fig. 2*C*) were calculated by integration. The integrated input is given in pC (1 pC is the electrical charge transferred, for example, by a 100 pA current for 10 ms). ***B***, Distributions of integrated mixed inputs to an L3 lamina I neuron. ***C***, The distribution of the integrated Aδ- and C-inputs, Aδ-inputs, and C-inputs centered on the segment where the neuron was located (0, vertical gray bar). More caudal and more rostral segmental dorsal roots are indicated by positive and negative numbers, respectively. ***D***, Comparison of the integrated mixed inputs to L4 lamina I and lamina II neurons from the strongest root (L5). The data for lamina I neurons ($n = 13$) are from ***A***, while those for lamina II neurons ($n = 19$) were obtained by reevaluation of recordings from Pinto et al. (2008b). SG, Substantia gelatinosa (lamina II).

microscope stage was aligned manually. The location of the neuronal soma and processes were determined on reconstructions of individual sections where borders of the gray and white matter were clearly identifiable. The two-dimensional serial sections were overlaid, aligned using the NeuroExplorer software (MBF Bioscience), and exported as bitmap images. Gray lines in Figures 6*B* and 9*B* indicate the contours of the bottom of the serial sections. For clarity, some contour lines were omitted.

Successful recovery was achieved in 14 cases for 10 lamina I neurons and 4 LSN neurons. In all these cases, the cell identification based on the fiber orientation was confirmed (Fig. 1*D*; see also Figs. 6*B*, 9*B*).

Recording. Whole-cell recordings from spinal sensory neurons (Melnick et al., 2004a,b; Szucs et al., 2009) were done in ACSF containing the following (in mM): NaCl 115, KCl 3, $CaCl_2$ 2, $MgCl_2$ 1, glucose 11, NaH_2PO_4 1, and $NaHCO_3$ 25 (pH 7.4 when bubbled with 95–5% mixture of O_2-CO_2). The amplifier was EPC10 (HEKA). The pipettes were pulled from thick-walled glass (BioMedical Instruments) and fire polished (resistance, 3–5 MΩ). The pipette solution contained the following (in mM): KCl 3, K-gluconate 150, $MgCl_2$ 1, BAPTA 1, and HEPES 10 (pH 7.3 adjusted with KOH, final $[K^+]$ was 161 mM). The signal was low-pass filtered at 2.9 kHz and sampled at 10 kHz. Offset potentials were compensated before seal formation. Liquid junction potentials were calculated and corrected for in all experiments using the compensation circuitry of the amplifier. The series resistance was 9–28 MΩ. Lamina I and LSN neurons were classified as tonic-firing neurons and delayed-firing neurons using criteria described previously for lamina II neurons (Santos et al., 2004, 2007). Tonic-firing neurons were able to support tonic firing during 500 ms depolarization induced by sustained current injection. In delayed-firing neurons, the first spikes typically appeared with a considerable time delay (200–500 ms) at the end of the depolarizing pulse and moved to its beginning as the stimulation increased. All numbers are given as mean ± SEM.

Stimulation of dorsal roots. Six unilateral roots (L1–L6) were stimulated as described previously (Pinto et al., 2008b). Each root was inserted into a suction electrode fabricated from borosilicate glass tube. The electrodes were fire polished to fit the size of the roots and mechanically fixed on a common holder. An isolated pulse stimulator (2100, A-M Systems) connected via a six-position switcher was used for a sequential stimulation of roots. Each suction pipette had its own reference electrode. Stimulation intensities used in these experiments did not evoke a cross-stimulation of roots by neighboring suction electrodes (Pinto et al., 2008b).

To evoke EPSCs in lamina I and LSN neurons, the roots were stimulated at intensities determined for complete recruitment of Aδ- and C-fibers in our previous study (Pinto et al., 2008a). With a 1 ms pulse, complete activation of both Aδ- and C-fiber-mediated compound action potential currents in isolated dorsal roots was reached at 50–150 μA (in most cases <100 μA) [see recruitment curve for C-fibers in Fig. 3*C*, control, from Pinto et al. (2008a)]. The present study was done using younger rats with thinner dorsal roots, and smaller currents (<100 μA) were sufficient for the fiber recruitment. Therefore, a 1 ms pulse of 100 μA was applied to completely activate both Aδ- and C-fiber EPSCs. For each neuron, at the beginning of the experiment, all roots were additionally tested at 150 μA to confirm that neither the number nor the magnitudes of EPSCs could be further increased. When the duration of the pulse (100 μA) was reduced to 50 μs, only the Aδ-component remained (see Fig. 2*B*,*C*). With one exception (Table 1, cell 14, root L4, conduction velocity 5.7 m/s), the monosynaptic Aδ-fiber EPSCs appeared with latencies corresponding to afferent conduction velocity of 0.41–4.4 m/s, which was within the range reported for the Aδ-component of the compound action potential current (Pinto et al., 2008a). The latencies of the C-fiber-mediated EPSCs corresponded to afferent conduction velocity below 0.55 m/s (Pinto et al., 2008a,b). The latencies were measured from the end of a 50 μs pulse for Aδ-fibers and from the middle point of a 1 ms pulse for C-fibers with a 1 ms allowance for synaptic transmission. The conduction distance included the length of the root from the opening of the suction electrode to the dorsal root entry zone and the estimated pathway within the spinal cord. Stimulus utilization time, i.e., the delay between the stimulus and beginning of the spike in the axon (Waddell et al., 1989), was not taken into account.

Classification of monosynaptic EPSCs. The EPSCs were evoked at frequencies allowing discrimination between the monosynaptic and polysynaptic inputs. These were the highest frequencies at which stable

Aδ- and C-fiber compound action potential currents could be evoked in the isolated dorsal roots (Pinto et al., 2008b). Based on those data, the Aδ-fiber-mediated EPSCs were considered as monosynaptic if the latency variation was <1 ms and there was no failure in 10 consecutive stimulations with 1 ms and 50 μs pulses at 1 Hz. The C-fiber-mediated EPSCs were considered as monosynaptic if there was no failure and the latency variation was <1 ms during 10 consecutive stimulations at 0.1 Hz. A root with multiple C- or Aδ-fiber inputs to a spinal neuron was considered as projecting monosynaptically if at least one EPSC was identified as monosynaptic. EPSCs that did not fulfill these criteria and all IPSCs were classified as polysynaptic. The EPSCs were recorded in lamina I and LSN neurons at −70 mV when IPSCs were small or not present. In the case of large polysynaptic IPSCs, the holding potential was changed to −80 mV ($E_{Cl} = -80$ mV). Analysis of polysynaptic inhibitory inputs was beyond the scope of this study.

Results

The following experiments were designed to study (1) the relative strength of monosynaptic and polysynaptic (mixed) inputs arising from different dorsal roots, (2) how the pattern of mixed inputs changes with segmental location of the spinal neuron, (3) whether the mixed inputs from several dorsal roots can evoke spikes in one neuron, and (4) whether Aδ- and C-fibers from different roots can converge monosynaptically onto single neurons.

Thirty-six lamina I neurons ($n = 19$, L4; $n = 17$, L3) and 16 LSN neurons ($n = 9$, L4; $n = 7$, L3) were tested for receiving inputs from the L1–L6 roots. To examine the change in the input pattern with location of the spinal neuron, recordings were done in two spinal cord segments, L4 and L3. The input resistances were 1.8 ± 0.2 GΩ ($n = 36$, lamina I) and 1.8 ± 0.3 GΩ ($n = 16$, LSN), respectively. The resting potentials measured with balanced amplifier input (Santos et al., 2004) were −63.8 ± 1.6 mV ($n = 36$, lamina I) and −62.0 ± 1.7 mV ($n = 16$, LSN).

Mixed inputs to lamina I neurons

Mixed inputs arising from six roots were analyzed in 23 lamina I neurons ($n = 13$, L4; $n = 10$, L3). In the remaining 13 cells, the analysis could not be done because of either discharge of voltage-gated Na^+ currents triggered by the EPSCs, damage of one of the six roots during the preparation, or deterioration of the recording conditions before the entire stimulation protocol could be completed.

Mixed inputs recorded in an L4 lamina I neuron are shown in Figure 2. First, each dorsal root was stimulated 5–15 times with a 1 ms pulse to elicit both Aδ- and C-fiber-mediated mixed EPSCs (Fig. 2*A*, upper traces), which were averaged for each dorsal root (lower traces). Then, each root was stimulated 5–15 times with a 50 μs pulse to elicit only Aδ-fiber-mediated mixed EPSCs (Fig. 2*B*, upper traces), which were also averaged (lower traces). The averaged traces are shown amplified and superimposed for each root (Fig. 2*C*). As expected, in most cases, the averaged Aδ-fiber input had a pronounced short-latency component, while the Aδ- and C-fiber input had both the short-latency (Aδ) and the long-latency (C) components.

To quantify the mixed inputs arising from individual roots, the area under the corresponding averaged traces was calculated by integration and resulting histograms are shown in Figure 3. The largest integrated Aδ- and C-fiber mixed input to an L4 lamina I neuron (Fig. 3*A*) ($n = 13$) arose from the dorsal root L5 (16.1 ± 4.9 pC), followed by L4 (8.1 ± 2.0 pC). The sum of all inputs from the L1–L6 roots was 39.5 ± 7.4 pC.

The Aδ-fiber mixed inputs (Fig. 3*A*) were smaller with the maximum value of 4.3 ± 0.7 pC obtained for the L5 root. The

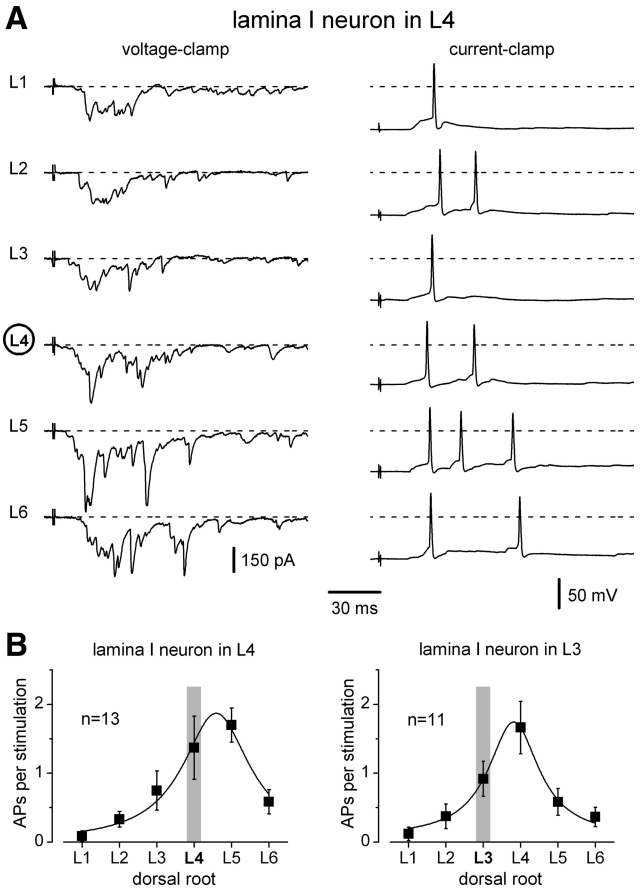

Figure 4. Efficacy of inputs to a lamina I neuron. ***A***, Voltage- and current-clamp recordings of synaptic inputs to an L4 lamina I neuron. Roots (L1–L6) were stimulated by 1 ms pulses to activate both Aδ- and C-fiber mixed EPSCs and EPSPs. The membrane potential was close to −70 mV. ***B***, The mean number of spikes evoked per stimulation of a root. For each neuron, each root was stimulated at least 10 times and the mean numbers were calculated. Graphs are based on data from 13 L4 lamina I neurons and 11 L3 lamina I neurons. Vertical gray bars indicate the segment of the neuron location. APs, action potentials.

C-fiber input was calculated as a difference between the corresponding integrated Aδ- and C-inputs and Aδ-inputs. The strongest C-fiber mixed input (Fig. 3*A*) also arose from the L5 root (11.8 ± 4.9 pC).

Similar measurements were done for L3 lamina I neurons (Fig. 3*B*) ($n = 10$). The strongest Aδ- and C-fiber mixed input was from the root L4 (12.5 ± 2.9 pC), followed by L3 (10.2 ± 3.0 pC). The sum of the Aδ- and C-fiber inputs from the L1–L6 roots was 35.9 ± 9.2 pC. The strongest Aδ-fiber inputs and C-fiber inputs to L3 lamina I neurons were also from the L4 root (Fig. 3*B*). The entire pattern of afferent input was shifted rostrally by one segment in comparison with that described for an L4 lamina I neuron.

The inputs to lamina I neurons located in different segments were summarized by centering them on the segment of the neuron location (Fig. 3*C*). Each centered distribution was obtained from 23 individual histograms normalized to 1. They also showed that the strongest mixed inputs arose from the root of the neighboring caudal segment (+1), followed by the root of the spinal segment of neuron location (0).

The non-NMDA receptor blocker CNQX (10 μM) completely suppressed inputs from 25 roots (data not shown; recovery, $n = 16$). The $GABA_A$ receptor blocker picrotoxin (100 μM) had no effect on the amplitudes of EPSCs evoked from the six dorsal root

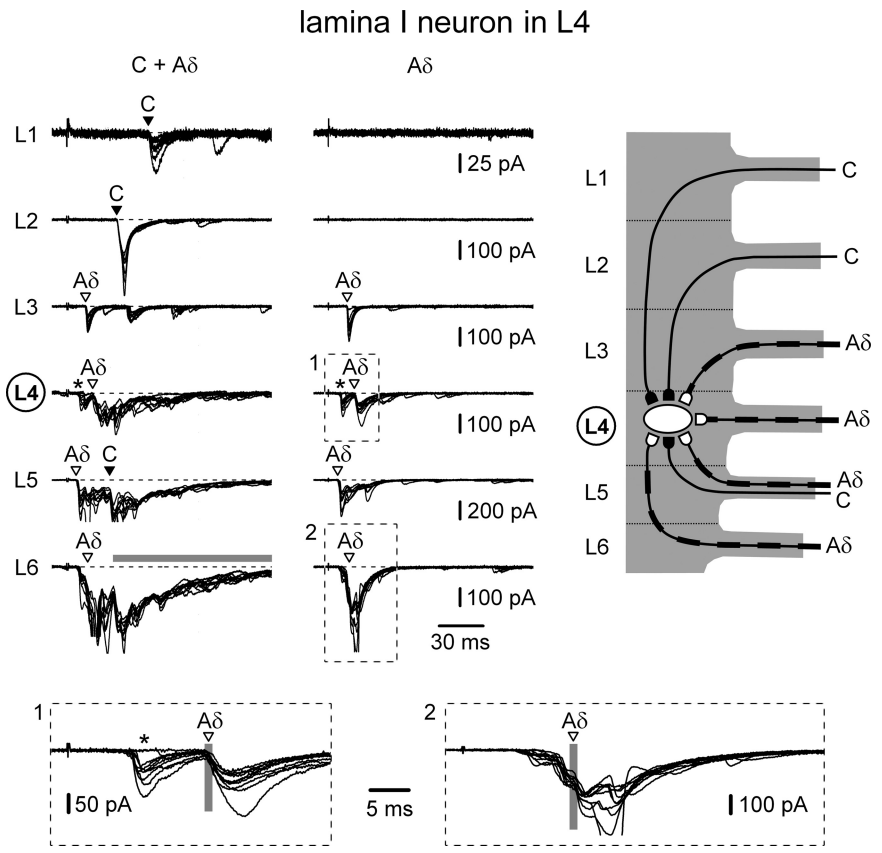

Figure 5. Converging monosynaptic Aδ- and C-fiber inputs to an L4 lamina I neuron. Recording from the lamina I neuron with the broadest input observed. Left, Recordings of EPSCs elicited by stimulating L1–L6 roots with 1 ms pulses. Holding potential, −70 mV. Monosynaptic C- and Aδ-fiber-mediated EPSCs are indicated by filled and open triangles, respectively. The triangles also show the time moment for which the latency analysis was done (see insets). Middle, The roots were also stimulated with 50 μs pulses. Recordings are shown as a superposition of 10 consecutive traces for roots with monosynaptic inputs (indicated by triangles) and 5 consecutive traces for roots without monosynaptic input. The C-fiber-mediated input from the L6 root (indicated by a horizontal gray bar) was too strong and could not be analyzed. Right, Schematic drawing of the monosynaptic projections of C- and Aδ-afferents originating from the L1–L6 roots to this L4 lamina I neuron. Insets at bottom show two examples of analysis of the monosynaptic inputs. Inset 1, EPSCs elicited by stimulating the L4 root at Aδ-fiber intensity. The faster component (marked by an asterisk) showing failures and the latency variation exceeding 1 ms was not considered as monosynaptic. The slower component (indicated by an open triangle) fulfilled criteria of monosynaptic input. The vertical gray bar has a width of 1 ms (maximum latency variation allowed for the monosynaptic response). Inset 2, The response to the L6 root stimulation consisted of multiple overlapping components of composite EPSC, one of which (indicated by an open triangle) was considered as monosynaptic. The triangle indicates the exact time moment for which the analysis was done. Note that here and in the following figures the triangles indicate the monosynaptic component, and therefore, may not coincide with the beginning of the composite EPSCs.

inputs in lamina 1 neurons ($n = 6$, data not shown), indicating that, under our conditions, GABAergic presynaptic inhibition (Wall and Bennett, 1994; Wall, 1995) did not reduce the inputs to the neurons.

Comparison with mixed inputs to lamina II neurons

To compare the integrated mixed inputs to lamina I and lamina II neurons, we reevaluated our data from Pinto et al. (2008b). In 19 lamina II neurons located in L4, the largest Aδ- and C-fiber input was from the root L5 (5.8 ± 1.4 pC), followed by the root L4 (2.9 ± 1.1 pC). The Aδ-fiber input (0.64 ± 0.26 pC, L5; 0.89 ± 0.52 pC, L4) was smaller than the C-fiber input (5.1 ± 1.4 pC, L5; 2.0 ± 0.9 pC, L4). The inputs to L4 lamina I and lamina II neurons from the strongest root (L5) are shown together in Figure 3*D*. The Aδ- and C-fiber inputs and the Aδ-inputs to lamina II neurons were significantly smaller than those to lamina I neurons ($p < 0.03$ and $p < 10^{-5}$, respectively, independent Student's t test), and while we had the impression that the C-fiber input was also smaller, the difference was not significant ($p = 0.14$, independent Student's t test).

Efficacy of mixed inputs to lamina I neurons

The physiological efficacy of the mixed inputs was studied in current-clamp mode in 24 lamina I neurons ($n = 13$, L4; $n = 11$, L3). The synaptic events were recorded at a preset membrane potential of −70 mV while the L1–L6 roots were stimulated to activate both Aδ- and C-fibers. In an L4 lamina I neuron shown in Figure 4*A*, stimulation of each of the six segmental dorsal roots could evoke spikes. In this particular neuron, the largest number of spikes (three) was elicited upon the stimulation of the L5 root. To quantify the efficacy of root stimulation in evoking spikes, we calculated the mean number of spikes activated per stimulation. For each neuron, each root was stimulated at least 10 times, and the mean numbers are plotted in Figure 4*B*. The most effective input with ~2 spikes per stimulation arose from the root of the neighboring caudal segment.

These results show that lamina I neurons receive mixed inputs from six dorsal roots. EPSPs from several roots can evoke postsynaptic spikes. The strongest input arises from the neighboring caudal segmental dorsal root. In the following experiments, we analyzed monosynaptic inputs.

Converging monosynaptic inputs to lamina I neurons

Of 36 lamina I neurons studied, 7 had only polysynaptic inputs, 1 had a monosynaptic input from only one root, and 8 showed large inputs with numerous overlapping EPSCs that could not be analyzed for their monosynaptic origin. In the remaining 20 neurons ($n = 11$, L4; $n = 9$, L3), it was possible to confirm the monosynaptic nature of inputs from several dorsal roots. Detailed description of these inputs is given in Table 1, where the neurons are arranged in order of decreasing dominance of Aδ- over C-fiber inputs. Since even in those neurons inputs from some roots were too strong to be analyzed (Table 1, asterisks), our data should be considered as an underestimate of the true number of converging roots onto single lamina I neurons.

The L1–L6 roots were first stimulated with 1 ms pulses (Fig. 5, left) and monosynaptic Aδ- and C-fiber-mediated EPSCs were identified on the basis of their stability and conduction velocity of the corresponding afferents (see Materials and Methods). The identification was confirmed by stimulating roots with 50 μs pulses (Fig. 5, middle); in all cases, the Aδ-fiber-mediated EPSCs remained, while the C-fiber-mediated EPSCs disappeared.

The L4 lamina I neuron shown in Figure 5 had the broadest monosynaptic primary afferent input (Table 1, cell 7). The L1 and

L2 root stimulations at 1 ms evoked monosynaptic C-fiber EPSCs (indicated by filled triangles), which disappeared with 50 μs stimulations. The input from the L3 root consisted of one monosynaptic Aδ-fiber EPSC (open triangle) and several polysynaptic C-fiber-range EPSCs. With 50 μs stimulation, only the monosynaptic Aδ-fiber EPSC persisted. Stimulation of the L4 root activated several Aδ-fiber EPSCs, one of which could be identified as monosynaptic. Input from the L5 root also contained several components; one Aδ- and one C-fiber-mediated EPSCs could be identified as monosynaptic. The input from the L6 root was the strongest. One Aδ-fiber EPSC component could be classified as monosynaptic. The C-fiber-mediated input (horizontal gray bar) consisted of numerous components, the majority of which could not be analyzed. The few of them that could be distinguished did not satisfy the criteria for a monosynaptic input. The soma and proximal dendrites of this neuron were labeled with biocytin, confirming its location in L4 lamina I (data not shown).

Thus, this lamina I neuron from the spinal segment L4 received monosynaptic Aδ-fiber inputs from the L3, L4, L5, and L6 segmental roots and monosynaptic C-fiber inputs from the L1, L2, and L5 roots (Fig. 5, right). The total converging monosynaptic input arose from six roots (L1–L6).

Recordings from an L3 lamina I neuron with dominating monosynaptic Aδ-fiber inputs are shown in Figure 6*A* (Table 1, cell 13). The neuron received converging monosynaptic Aδ-afferent inputs from the L3, L4, and L5 roots (Fig. 6*A*, right). This neuron was labeled with biocytin and recovery was achieved for the dendrites and the axon (Fig. 6*B*). The rounded soma was located in the lateral part of the marginal zone in the L3 segment and some of the dendrites reached deeper laminae of the dorsal horn. These characteristics made it similar to the type IIB multipolar neuron described by Lima and Coimbra (1986). The axon had local collaterals around the cell body and one prominent caudally oriented branch, which gave rise to faint collaterals that could not be followed. No ventrally oriented branch of this axon could be detected.

Thus, thin afferents from up to six dorsal roots can converge monosynaptically onto individual lamina I neurons and each neuron can receive inputs from both Aδ- and C-fibers.

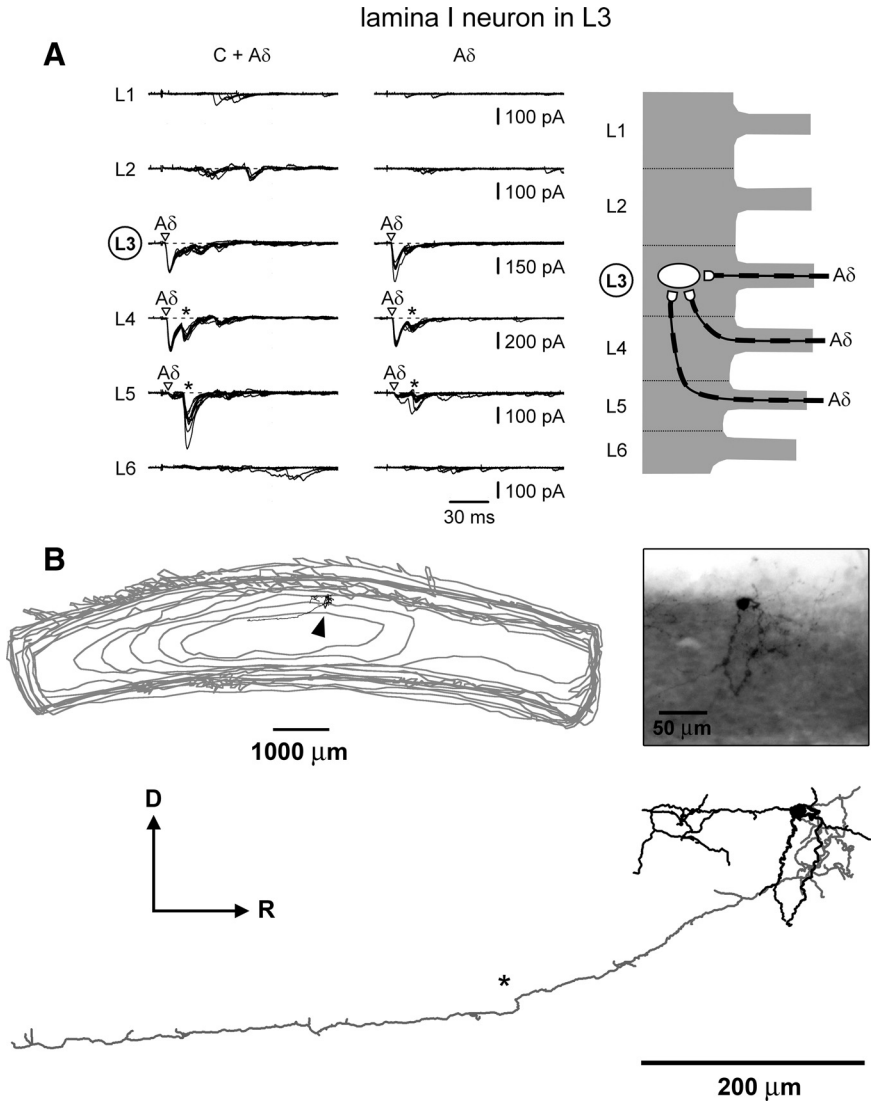

Figure 6. Converging monosynaptic Aδ-fiber inputs to an L3 lamina I neuron. ***A***, Left, EPSCs elicited by stimulating L1–L6 roots with 1 ms pulses. Holding potential, −70 mV. Monosynaptic Aδ-fiber EPSCs are indicated by open triangles. Middle, The roots were stimulated at 50 μs. Recordings are shown as a superposition of 10 and 5 consecutive traces for roots with and without monosynaptic inputs, respectively. Inputs from the roots L4 and L5 also show composite EPSCs (indicated by asterisks) consisting of overlapping slow Aδ- and fast C-fiber components. In these composite EPSCs, neither the C-fiber component (analyzed at 1 ms stimulation) nor the-Aδ-fiber component (analyzed at 1 ms and 50 μs stimulations) satisfied our criteria for monosynaptic inputs. Right, Schematic drawing of the monosynaptic Aδ-fibers projecting from the L3, L4, and L5 dorsal roots to this L3 lamina I neuron. ***B***, Biocytin-labeled soma, axon, and dendrites of the lamina I neuron from ***A***. The axon had local collaterals around the cell body and one prominent caudally oriented branch (indicated by an asterisk), which gave rise to faint collaterals. Gray lines indicate the contours of the bottom of the serial sections (some contour lines were omitted).

Mixed inputs to LSN neurons

Inputs from the L1–L6 roots were also recorded in 11 LSN neurons (Fig. 7*A*). The overall input was weaker than in lamina I neurons. For an L4 LSN neuron (Fig. 7*B*) ($n = 6$), the sum of the Aδ- and C-fiber mixed inputs from the six roots was 18.7 ± 7.6 pC. The strongest root (L5) and the root of the neuron segment (L4) contributed 6.4 ± 2.8 pC and 3.4 ± 1.1 pC, respectively. For an L3 LSN neuron ($n = 5$, data not shown), the sum of the Aδ- and C-fiber inputs from all roots was 29.7 ± 8.6 pC, with 6.5 ± 3.2 pC arising from the strongest root (L5) and 6.4 ± 0.8 pC from the root of the neuron segment (L3). The centered distribution for all LSN neurons (Fig. 7*C*) showed that the strongest mixed input was from the root of the neighboring caudal segment.

The efficacy of the inputs was studied in four LSN neurons ($n = 2$, L4; $n = 2$, L3). The roots were stimulated to activate both Aδ- and C-fiber EPSPs. An L4 LSN neuron shown in Figure 8*A* responded with spikes to stimulation of five different roots. However, the efficacy of root stimulation in evoking spikes in LSN

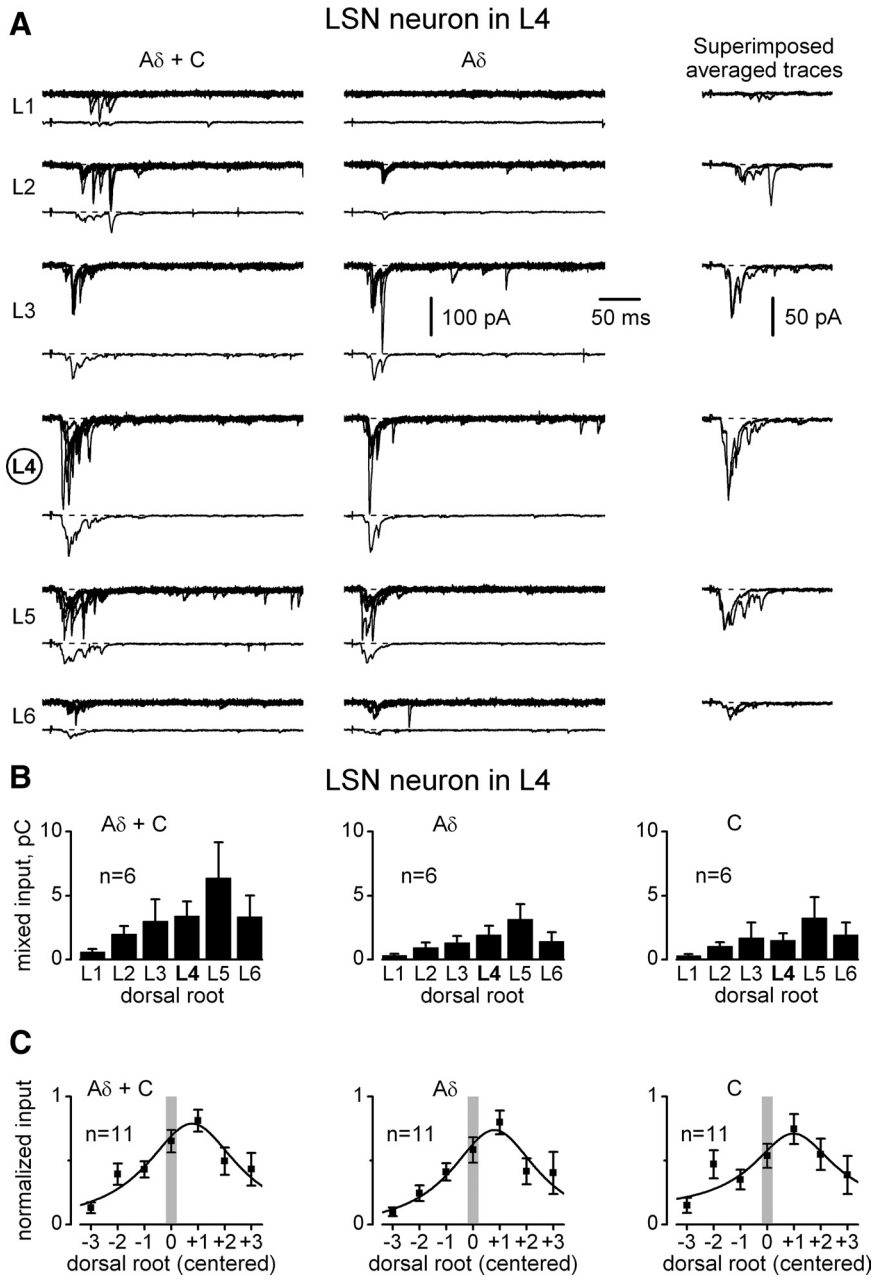

Figure 7. Aδ- and C-fiber mixed inputs to an LSN neuron. ***A***, Mixed EPSCs elicited in an L4 LSN neuron by stimulating L1–L6 roots. The stimulation protocol was as in Figure 2. Holding potential, −70 mV. ***B***, Integrated mixed inputs to an L4 LSN neuron. ***C***, Centered mixed inputs to an LSN neuron. Pooled data from L4 LSN neurons ($n = 6$) and L3 LSN neurons ($n = 5$).

neurons was lower than in lamina I neurons. The mixed inputs from the root of the neuron segment evoked 0.35 ± 0.26 spikes per stimulation, from the neighboring caudal root 1.1 ± 0.4 spikes per stimulation and from the neighboring rostral root 0.30 ± 0.18 spikes per stimulation ($n = 4$; pooled data for the L4 and L3 LSN neurons). Thus again, the most effective input was from the neighboring caudal segmental root.

CNQX (10 μM) completely blocked inputs from 14 roots (data not shown; recovery, $n = 10$). Picrotoxin (100 μM) did not increase the amplitude of EPSCs evoked by stimulating the L1–L6 roots in 2 LSN neurons tested.

Since, to our knowledge, there are no descriptions of the membrane properties of LSN neurons, the patterns of their intrinsic firing were also recorded. LSN neurons ($n = 16$) were hyperpolarized or depolarized from a preset membrane potential of −70 mV by injecting 500 ms current pulses (Fig. 8*B*). Depolarizing current pulses of 5–15 pA were sufficient to evoke discharges in the neurons. Tonic-firing pattern was found to be typical for LSN neurons ($n = 16$). In 14 of 16 LSN neurons, we also observed a typical slow afterhyperpolarization preceded by a fast afterhyperpolarization (Fig. 8*C*).

Thus, LSN neurons receive Aδ- and C-afferent mixed inputs from all six dorsal roots and the inputs from several roots can evoke spikes. The LSN neurons typically show a tonic pattern of firing.

Converging monosynaptic inputs to LSN neurons

In 7 LSN neurons (4 from L4 and 3 from L3), it was possible to analyze monosynaptic inputs (Table 2). In general, the number of monosynaptically converging roots was lower than for lamina I neurons (Tables 1, 2). An L3 LSN neuron shown in Figure 9*A* (Table 2, cell 5) received monosynaptic Aδ-fiber-mediated inputs from the segmental roots L3 and L4. All inputs from the L1, L2, and L6 roots were polysynaptic. The Aδ-fiber inputs from the L5 root could not be analyzed because of high activity of multiple components (indicated by horizontal gray bars). This LSN neuron was labeled with biocytin, and recovery was achieved for its dendrites and the axon (Fig. 9*B*). The large cell body was located inside the dorsolateral funiculus (Fig. 9*B*, photograph) adjacent to the lateral border of the dorsal gray matter. The soma gave rise to four major dendrites with no specific orientation and only a few branches along their course. The axon of this neuron gave rostrocaudal and ventral collaterals with numerous varicosities. The main axon descended ventrally and medially and crossed the level of the central canal. The course of the main axon toward the contralateral anterolateral white matter indicated that this cell is likely to be a projection neuron (Mehler et al., 1960; Dostrovsky and Craig, 2006).

It was possible to conclude that LSN neurons receive converging monosynaptic inputs from both Aδ- and C-afferents from L2–L6 roots (Table 2). The axon organization of the LSN neuron allows it to project the multisegmental input to both the spinal gray matter and supraspinal centers.

Discussion

Mixed monosynaptic and polysynaptic inputs

We have shown that individual lamina I and LSN neurons can receive mixed (monosynaptic and polysynaptic) inputs from as many as six dorsal roots. The pattern of the afferent supply shifts with the segmental location of the neuron in the spinal cord. For

both lamina I and LSN neurons, the strongest input arose from the root of the neighboring caudal segment, followed by the root of the segment of the neuron. In agreement with this, stimulation of the neighboring caudal root was most effective in evoking spikes. Mixed inputs from up to six roots can be sufficiently strong to evoke spikes in a lamina I neuron. Therefore, our data suggest that both lamina I and LSN neurons are involved in the intersegmental integration of the primary afferent input. It should be noted that our stimulation protocol was applied to only 6 roots and it is possible that even more distal inputs could be found if more remote roots had been studied. Besides, the integration pattern described here for young rats may be more (or less) complex in adult animals.

With one exception (see Materials and Methods), the EPSCs were mediated by afferents with conduction velocities in the Aδ- and C-fiber range (<4.4 m/s) (Pinto et al., 2008a), indicating that the neurons studied were involved in nociceptive processing. The remaining EPSC might be mediated by one of those Aδ-fibers (conduction velocity, 5.7 m/s) that contribute to the region of the compound action potential current where Aδ- and Aβ-waves overlap (Pinto et al., 2008a).

The overall mixed input to lamina I neurons was stronger than that to lamina II neurons. In part, this difference might be explained by a possible cut of the lateral portion of the dendritic tree of lamina II neurons in the preparation used by Pinto et al. (2008b). The Aδ-input was much stronger in lamina I neurons (Fig. 3*D*), which are likely to be the principal targets of Aδ-afferents. Surprisingly, the mixed C-fiber input was also larger in lamina I neurons. This may imply that lamina I integrates both its direct C-fiber input and the C-fiber input to lamina II transmitted via excitatory interneuron pathways to lamina I (Santos et al., 2007; Kato et al., 2009).

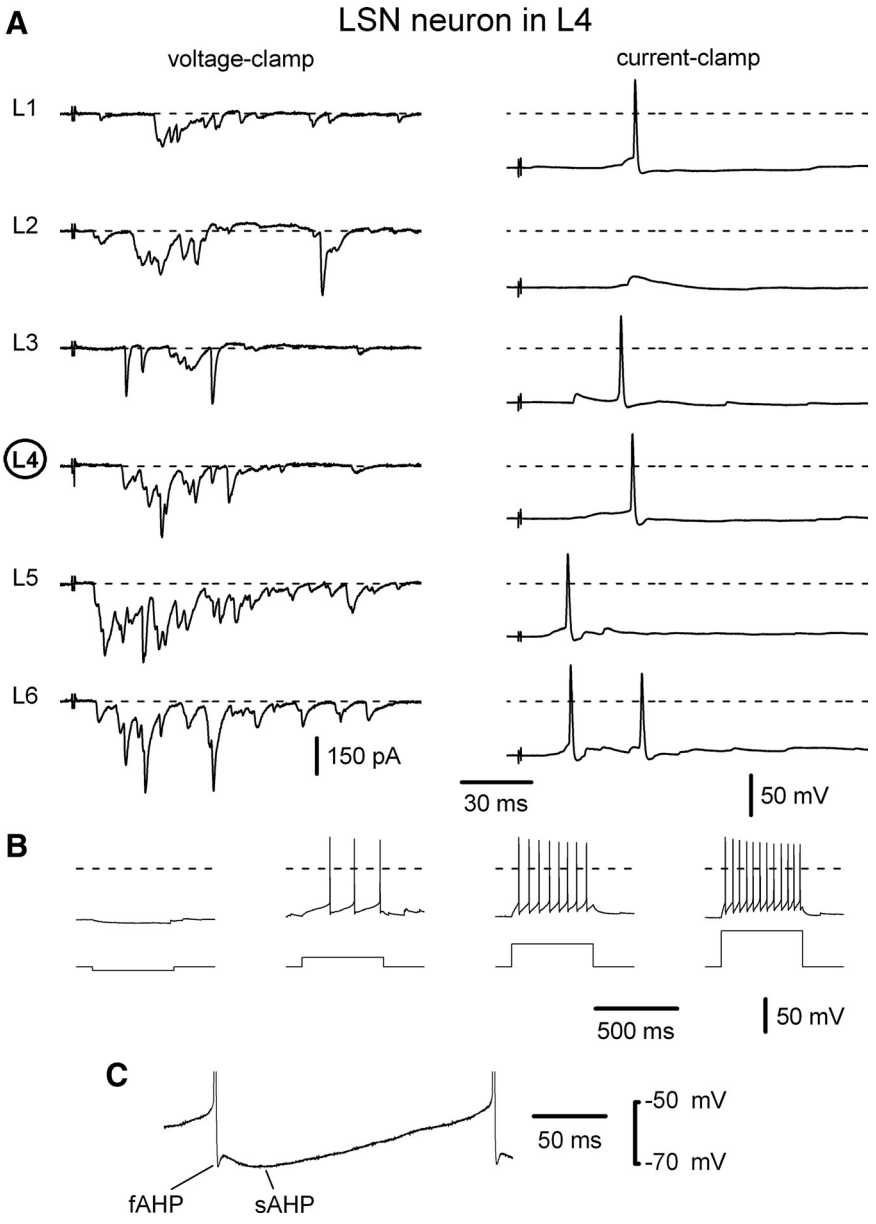

Figure 8. Efficacy of inputs to an LSN neuron. ***A***, Voltage- and current-clamp recordings of synaptic inputs to an L4 LSN neuron. The L1–L6 roots were stimulated by 1 ms pulses to activate both Aδ- and C-fiber mixed EPSCs and EPSPs. Stimulation of five roots evoked spikes. The membrane potential was −70 mV. ***B***, Membrane responses of an LSN neuron to an injection of 500 ms current pulses of −5 pA, +15 pA, +35 pA, and +55 pA. ***C***, A fast afterhyperpolarization (fAHP) and a slow afterhyperpolarization (sAHP) observed in the majority of LSN neurons.

Table 2. Converging monosynaptic inputs to LSN neurons in L4 and L3

	L1		L2		L3		L4		L5		L6			
Cell	Aδ	C	Aδ	C	Aδ	C	Aδ	C	Aδ	C	Aδ	C	Input from roots	Converging roots
LSN neuron in L4														
1	—	—	○	—	—	—	○	—	○	*	*	*	3Aδ	3
2	*	—	*	—	—	●	—	*	*	*	○	—	1Aδ + 1C	2
3	—	—	—	●	*	*	—	—	○	*	—	—	1Aδ + 1C	2
4	—	—	—	●	—	—	*	*	*	*	—	●	2C	2
LSN neuron in L3														
5	—	—	—	—	○	—	○	—	*	—	—	—	2Aδ	2
6	—	—	○	●	○	—	*	●	—	—	—	—	2Aδ + 2C	3
7	—	—	*	*	*	*	*	*	—	●	—	●	2C	2

The table describes those LSN neurons for which the monosynaptic inputs from at least two segmental dorsal roots were confirmed. The same symbols are used as in Table 1.

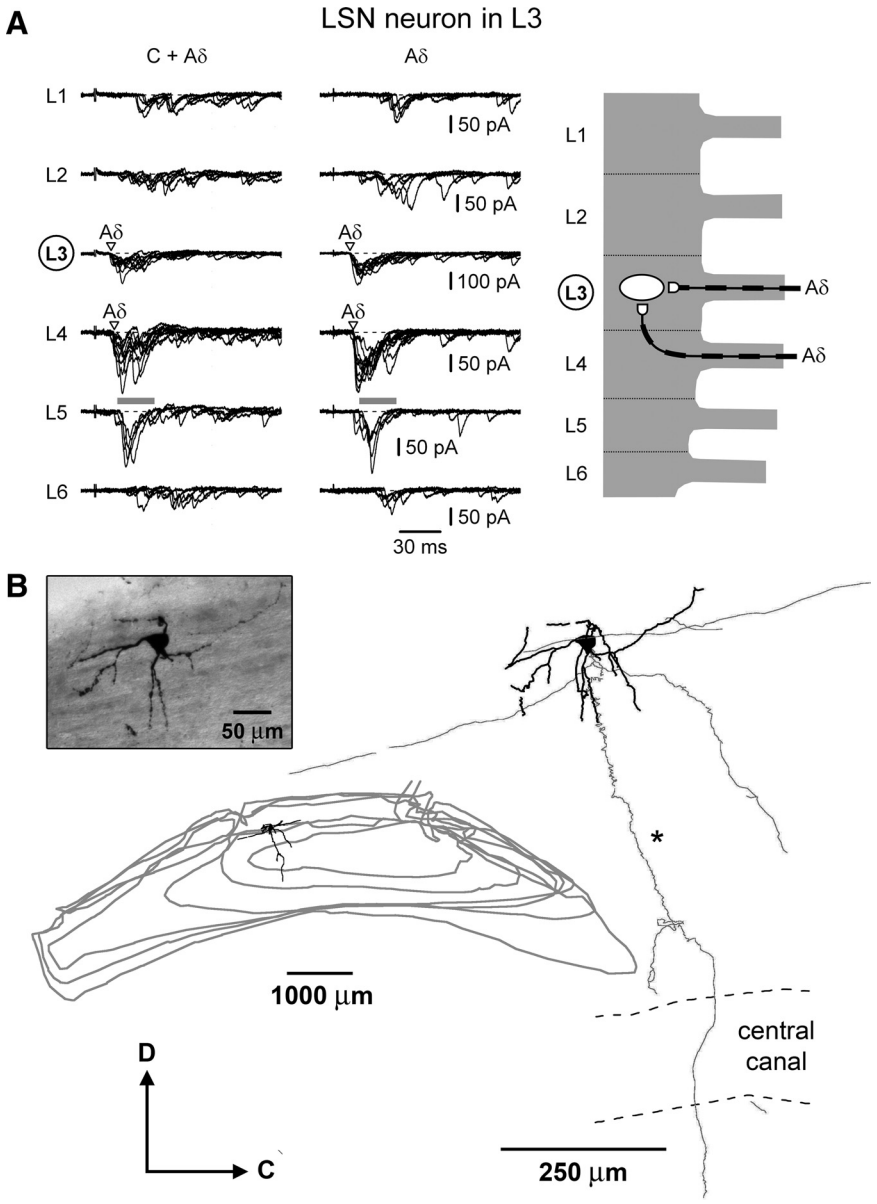

Figure 9. Converging monosynaptic Aδ-fiber inputs to an L3 LSN neuron. ***A***, Left, EPSCs elicited by stimulating L1–L6 roots (1 ms pulses). Holding potential, −80 mV. Monosynaptic Aδ-fiber EPSCs are indicated by open triangles. Middle, The roots were stimulated with short pulses (50 μs). Recordings are shown as a superposition of 10 and 5 consecutive traces for the roots with and without monosynaptic inputs, respectively. Right, Schematic drawing of the monosynaptic Aδ-fibers projecting from the L3 and L4 roots to this L3 LSN neuron. ***B***, Biocytin-labeled soma, axon, and dendrites of the neuron from ***A***. The soma located inside the dorsolateral funiculus gave rise to four major dendrites. The axon gave rostrocaudal and ventral collaterals with numerous en-passant varicosities. The main axon (indicated by an asterisk) had constant diameter and descended ventrally and medially in several sections before crossing the level of the central canal toward the contralateral anterolateral white matter. Gray lines indicate the contours of the bottom of the serial sections (some contour lines were omitted).

Converging multisegmental monosynaptic inputs

Lamina I neurons can receive monosynaptic input from six different segmental roots. This input was broader than in lamina II neurons, where it arises from two to four roots (Pinto et al., 2008b). We identified higher percentage of lamina I neurons that exhibited the monosynaptic Aδ-fiber inputs (Table 1), while the monosynaptic C-fiber inputs were more frequently seen in lamina II neurons [Pinto et al. (2008b), their Table 1].

Broad monosynaptic inputs to a lamina I neuron imply several-segment-long spinal branches of thin afferents. Anatomical studies had shown that the central branches of thin afferents entering the superficial dorsal horn terminate not only in the segment of root entrance but also one to two segments above and below (Szentagothai, 1964; Cruz et al., 1987). Physiological studies reported monosynaptic C-fiber-mediated responses in lamina II neurons located two (Kato et al., 2004; Pinto et al., 2008b) or, at most, three segments away from the root entrance segment (Pinto et al., 2008b). The most distant monosynaptic Aδ- and C-afferent inputs to lamina I neurons recorded here were also from the roots entering three segments away from the segment of the neuron location (Table 1, cells 1, 7, and 16).

LSN neurons receive monosynaptic projections from both Aδ- and C-afferents originating from up to three roots. They can integrate multisegmental root inputs for projection to supraspinal centers (Menétrey et al., 1982; Pechura and Liu, 1986; Menétrey and Basbaum, 1987; Leah et al., 1988; Burstein et al., 1990a,b) and via axon collaterals to the spinal gray matter (Olave and Maxwell, 2004). Our data support the idea of involvement of LSN neurons in nociceptive processing (Olave and Maxwell, 2004). Converging inputs to LSN neurons can be from afferents innervating joints and deep tissue (Menétrey et al., 1980), muscles (Olave and Maxwell, 2004), and viscera (Sugiura et al., 1989).

Monosynaptic somatosensory integration on a lamina I neuron

Broad monosynaptic input to lamina I neurons in L4–L3 may imply their involvement in spinal somatosensory integration. Indeed, lamina I receives thin afferents innervating different somatic (skin, muscles, and joints) structures (Dostrovsky and Craig, 2006). These afferents differ in their numbers and segmental distribution within the spinal cord, however, as the following analysis shows, those innervating one particular type of structure are unlikely to provide the extent of the monosynaptic input reported here.

Afferents supplying joints form <5% of the somatic afferents (Swett et al., 1991). In the remaining population, the ratio of the thin afferents innervating skin to those supplying muscles is 11 to 1 (Swett et al., 1991) (76% of cutaneous DRG neurons, 69% of which were small vs 19% of the muscle-innervating DRG neurons, 25% of which were small). Thus, cutaneous afferents far outnumber those innervating other structures, and therefore, provide major monosynaptic Aδ- and C-fiber input to lamina I neurons. The afferents supplying different somatic structures enter the spinal cord through several segmental roots, analysis of which is presented in Table 3.

Cutaneous inputs to laminae I–II have rigorous somatotopic organization (Willis and Coggeshall, 1978; Amaral, 2000). For

Table 3. Involvement of the lumbar dorsal roots in somatic innervation

	Skin[a]								Muscle		Joint			
DRG/root	Ankle, medial (P7)	Ankle, dorsal (P14)	Paw, medial (P8)	Paw, lateral (P12)	Digit I, ventral (P10)	Digit V, ventral (P11)	Sole, center (P9)	Hip (P19)	Lower back muscle[c]	Leg muscles[b]	L5/6 facet[d]	Hip[e]	Knee[c]	Ankle[b]
L1									●		●	●	●	
L2									●	●	●	●	●	●
L3	●	●	●		●			●	●	●	●	●	●	●
L4	●	●	●	●	●	●	●	●	●	●	●	●	●	●
L5	●	●	●	●	●	●	●	●		●	●	●		●
L6				●				●						

This table is based on studies using different labeling techniques. [a]Takahashi et al. (2003), [c]Ohtori et al. (2003), [d]Ohtori et al. (2000), and [e]Nakajima et al. (2008) used peripheral injection of a retrograde tracer that labeled cells in several DRGs. A segmental dorsal root was considered as projecting to the spinal cord (filled circle) if the number of labeled cells in the corresponding DRG was >2.0% of the total number of labeled cells in all DRGs. [b]Pinter and Szolcsanyi (1995) identified segmental dorsal roots supplying muscles and joints by the plasma extravasation technique. All eight cutaneous reference points had their identified single projection fields in the superficial dorsal horn of the L4 or L3 segment. Their corresponding numbers were taken from Takahashi et al. (2003). Our lamina I neurons were located in L3 and L4.

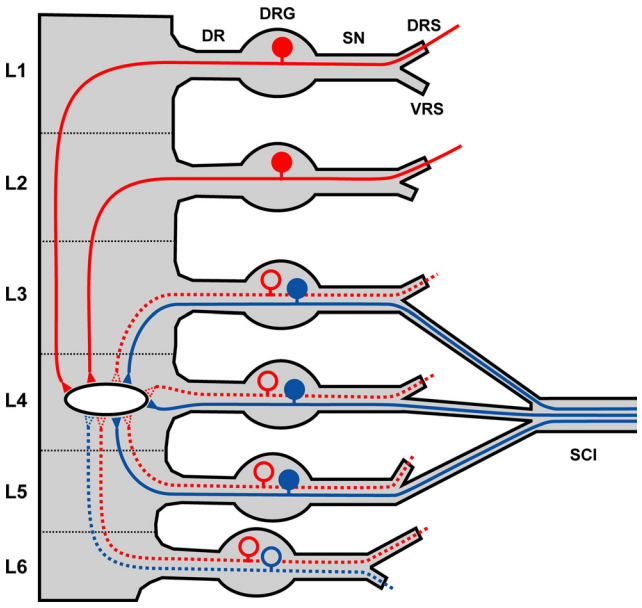

Figure 10. Proposed model of monosynaptic convergence of thin afferents onto a lamina I neuron. A model of inputs to an L4 lamina I neuron from the L1–L6 roots was developed on the basis of our data and studies described in Table 3. Solid and dotted lines indicate the most probable and less probable types of afferents, respectively. Cutaneous afferents (blue) originating from the sciatic nerve provide the major supply of an L4 lamina I neuron from the L3, L4, and L5 roots. The monosynaptic projections to an L4 lamina I neuron arising from the L1 and L2 roots are of noncutaneous somatic (muscles and joints) origin (red). DR, Dorsal root; SN, spinal nerve; DRS, dorsal ramus of the spinal nerve; VRS, ventral ramus of the spinal nerve; SCI, sciatic nerve.

segments L4 and L3, cutaneous afferent projections were mapped by transganglionic tracing methods, which revealed the superficial dorsal horn regions where neurons can receive monosynaptic inputs. It was found that the specific cutaneous areas innervated by different branches of a peripheral nerve project to their separate and distinct regions in the superficial dorsal horn (Swett and Woolf, 1985; Takahashi et al., 2003). Therefore, an L4–L3 lamina I neuron located in the projection field of sciatic nerve (Swett and Woolf, 1985) can receive monosynaptic cutaneous inputs only from the roots forming this nerve, L3–L6 (mostly from L4–L5) (Swett et al., 1991). Similarly, an L3 lamina I neuron from the projection field of saphenous nerve can only receive monosynaptic cutaneous inputs from more rostral L3–L2 roots (Swett and Woolf, 1985). In agreement with this, thin afferents innervating cutaneous reference points with single representation fields in the L4 and L3 segments were shown to enter the spinal cord through two to four roots (L3–L6) (Table 3) (Takahashi et al., 2003). Thus, monosynaptic cutaneous inputs to a lamina I neuron from six roots appear to be unlikely.

To our knowledge, there is no detailed description of projections of the noncutaneous reference points to the superficial laminae. However, a number of studies described a contribution of the lumbar roots or dorsal root ganglia (DRGs) to the innervation of muscles and joints (Table 3). The afferents innervating the low back or leg muscles were found in four lumbar roots including L1 (Pintér and Szolcsányi, 1995; Ohtori et al., 2003). The afferents originating from joints enter the spinal cord through, probably, the broadest range of the lumbar dorsal roots (Pintér and Szolcsányi, 1995; Ohtori et al., 2000, 2003; Nakajima et al., 2008). For example, the L5/6 facet joint is innervated by five DRGs, three of which (L3–L5) innervate segmentally and two (L1–L2) nonsegmentally through the paravertebral sympathetic trunk (Ohtori et al., 2000). Thus, a noncutaneous reference point also cannot project to a lamina I neuron through six segmental roots. Furthermore, low percentages of muscular or joint afferents in peripheral nerves (Swett et al., 1991) make them unlikely candidates for the majority of converging inputs in Table 1.

Therefore, the most plausible interpretation of our results is involvement of lamina I neurons in somatosensory integration. Monosynaptic cutaneous inputs from the L3–L6 roots (supplied via sciatic nerve) can be directly integrated with muscular or joint inputs from the L1–L6 roots (Fig. 10). This monosynaptic integration of somatosensory inputs on a lamina I neuron may underlie neurological phenomena of referred pain originating from the musculoskeletal structures.

In conclusion, we have shown that lamina I and LSN neurons receive broad intersegmental monosynaptic inputs from Aδ- and C-fibers. Lamina I neurons may function as integrators of somatosensory inputs at the spinal cord level.

References

Amaral DG (2000) The functional organization of perception and movement. In: Principles of neural science (Kandel ER, Schwartz JH, Jessell TM, ed), Ed 4, pp 337–348. New York: McGraw-Hill.

Burstein R, Cliffer KD, Giesler GJ Jr (1990a) Cells of origin of the spinohypothalamic tract in the rat. J Comp Neurol 291:329–344.

Burstein R, Dado RJ, Giesler GJ Jr (1990b) The cells of origin of the spinothalamic tract of the rat: a quantitative reexamination. Brain Res 511:329–337.

Cervero F, Connell LA (1984a) Distribution of somatic and visceral primary afferent fibers within the thoracic spinal cord of the cat. J Comp Neurol 230:88–98.

Cervero F, Connell LA (1984b) Fine afferent fibers from viscera do not terminate in the substantia gelatinosa of the thoracic spinal cord. Brain Res 294:370–374.

Cruz F, Lima D, Coimbra A (1987) Several morphological types of terminal arborizations of primary afferents in laminae I–II of the rat spinal cord, as

shown after HRP labeling and Golgi impregnation. J Comp Neurol 261:221–236.

Dostrovsky JO, Craig AD (2006) Ascending projection systems. In: Wall and Melzack's textbook of pain (McMahon SB, Koltzenburg M, ed), Ed 5, pp 187–203. Philadelphia: Elsevier Churchill Livingstone.

Giesler GJ Jr, Urca G, Cannon JT, Liebeskind JC (1979) Response properties of neurons of the lateral cervical nucleus in the rat. J Comp Neurol 186:65–77.

Gwyn DG, Waldron HA (1968) A nucleus in the dorsolateral funiculus of the spinal cord of the rat. Brain Res 10:342–351.

Gwyn DG, Waldron HA (1969) Observations on the morphology of a nucleus in the dorsolateral funiculus of the spinal cord of the guinea-pig, rabbit, ferret and cat. J Comp Neurol 136:233–236.

Kato G, Furue H, Katafuchi T, Yasaka T, Iwamoto Y, Yoshimura M (2004) Electrophysiological mapping of the nociceptive inputs to the substantia gelatinosa in rat horizontal spinal cord slices. J Physiol 560:303–315.

Kato G, Kawasaki Y, Koga K, Uta D, Kosugi M, Yasaka T, Yoshimura M, Ji RR, Strassman AM (2009) Organization of intralaminar and translaminar neuronal connectivity in the superficial spinal dorsal horn. J Neurosci 29:5088–5099.

Kumazawa T, Perl ER (1978) Excitation of marginal and substantia gelatinosa neurons in the primate spinal cord: indications of their place in dorsal horn functional organization. J Comp Neurol 177:417–434.

Leah J, Menétrey D, de Pommery J (1988) Neuropeptides in long ascending spinal tract cells in the rat: evidence for parallel processing of ascending information. Neuroscience 24:195–207.

Lima D, Almeida A (2002) The medullary dorsal reticular nucleus as a pronociceptive centre of the pain control system. Prog Neurobiol 66:81–108.

Lima D, Coimbra A (1986) A Golgi study of the neuronal population of the marginal zone (lamina I) of the rat spinal cord. J Comp Neurol 244:53–71.

Mehler WR, Feferman ME, Nauta WJ (1960) Ascending axon degeneration following anterolateral cordotomy. An experimental study in the monkey. Brain 83:718–750.

Melnick IV, Santos SF, Safronov BV (2004a) Mechanism of spike frequency adaptation in substantia gelatinosa neurones of rat. J Physiol 559: 383–395.

Melnick IV, Santos SF, Szokol K, Szûcs P, Safronov BV (2004b) Ionic basis of tonic firing in spinal substantia gelatinosa neurons of rat. J Neurophysiol 91:646–655.

Menétrey D, Basbaum AI (1987) Spinal and trigeminal projections to the nucleus of the solitary tract: a possible substrate for somatovisceral and viscerovisceral reflex activation. J Comp Neurol 255:439–450.

Menétrey D, Chaouch A, Besson JM (1980) Location and properties of dorsal horn neurons at origin of spinoreticular tract in lumbar enlargement of the rat. J Neurophysiol 44:862–877.

Menétrey D, Chaouch A, Binder D, Besson JM (1982) The origin of the spinomesencephalic tract in the rat: an anatomical study using the retrograde transport of horseradish peroxidase. J Comp Neurol 206:193–207.

Nakajima T, Ohtori S, Yamamoto S, Takahashi K, Harada Y (2008) Differences in innervation and innervated neurons between hip and inguinal skin. Clin Orthop Relat Res 466:2527–2532.

Ohtori S, Takahashi K, Chiba T, Yamagata M, Sameda H, Moriya H (2000) Substance P and calcitonin gene-related peptide immunoreactive sensory DRG neurons innervating the lumbar facet joints in rats. Auton Neurosci 86:13–17.

Ohtori S, Takahashi K, Chiba T, Yamagata M, Sameda H, Moriya H (2003) Calcitonin gene-related peptide immunoreactive neurons with dichotomizing axons projecting to the lumbar muscle and knee in rats. Eur Spine J 12:576–580.

Olave MJ, Maxwell DJ (2004) Axon terminals possessing alpha2C-adrenergic receptors densely innervate neurons in the rat lateral spinal nucleus which respond to noxious stimulation. Neuroscience 126: 391–403.

Pechura CM, Liu RP (1986) Spinal neurons which project to the periaqueductal gray and the medullary reticular formation via axon collaterals: a double-label fluorescence study in the rat. Brain Res 374:357–361.

Pintér E, Szolcsányi J (1995) Plasma extravasation in the skin and pelvic organs evoked by antidromic stimulation of the lumbosacral dorsal roots of the rat. Neuroscience 68:603–614.

Pinto V, Derkach VA, Safronov BV (2008a) Role of TTX-sensitive and TTX-resistant sodium channels in Adelta- and C-fiber conduction and synaptic transmission. J Neurophysiol 99:617–628.

Pinto V, Szûcs P, Derkach VA, Safronov BV (2008b) Monosynaptic convergence of C- and Adelta-afferent fibers from different segmental dorsal roots on to single substantia gelatinosa neurones in the rat spinal cord. J Physiol 586:4165–4177.

Safronov BV, Pinto V, Derkach VA (2007) High-resolution single-cell imaging for functional studies in the whole brain and spinal cord and thick tissue blocks using light-emitting diode illumination. J Neurosci Methods 164:292–298.

Santos SF, Melnick IV, Safronov BV (2004) Selective postsynaptic inhibition of tonic-firing neurons in substantia gelatinosa by mu-opioid agonist. Anesthesiology 101:1177–1183.

Santos SF, Rebelo S, Derkach VA, Safronov BV (2007) Excitatory interneurons dominate sensory processing in the spinal substantia gelatinosa of rat. J Physiol 581:241–254.

Sugiura Y, Terui N, Hosoya Y (1989) Difference in distribution of central terminals between visceral and somatic unmyelinated (C) primary afferent fibers. J Neurophysiol 62:834–840.

Swett JE, Woolf CJ (1985) The somatotopic organization of primary afferent terminals in the superficial laminae of the dorsal horn of the rat spinal cord. J Comp Neurol 231:66–77.

Swett JE, Torigoe Y, Elie VR, Bourassa CM, Miller PG (1991) Sensory neurons of the rat sciatic nerve. Exp Neurol 114:82–103.

Szentagothai J (1964) Neuronal and synaptic arrangement in the substantia gelatinosa rolandi. J Comp Neurol 122:219–239.

Szucs P, Pinto V, Safronov BV (2009) Advanced technique of infrared LED imaging of unstained cells and intracellular structures in isolated spinal cord, brainstem, ganglia and cerebellum. J Neurosci Methods 177: 369–380.

Takahashi Y, Chiba T, Kurokawa M, Aoki Y (2003) Dermatomes and the central organization of dermatomes and body surface regions in the spinal cord dorsal horn in rats. J Comp Neurol 462:29–41.

Waddell PJ, Lawson SN, McCarthy PW (1989) Conduction velocity changes along the processes of rat primary sensory neurons. Neuroscience 30:577–584.

Wall PD (1995) Do nerve impulses penetrate terminal arborizations? A presynaptic control mechanism. Trends Neurosci 18:99–103.

Wall PD, Bennett DL (1994) Postsynaptic effects of long-range afferents in distant segments caudal to their entry point in rat spinal cord under the influence of picrotoxin or strychnine. J Neurophysiol 72:2703–2713.

Willis WD, Coggeshall RE (1978) Sensory mechanisms of the spinal cord. New York: Wiley.

Woolf CJ, Fitzgerald M (1983) The properties of neurones recorded in the superficial dorsal horn of the rat spinal cord. J Comp Neurol 221:313–328.